Electronic Supplementary Information

Novel Aluminum-BODIPY Diads: Intriguing Dual-Emission via Photoinduced Energy Transfer

Changho Sohn,[a] Jisu Jeong,[b] Ji Hye Lee,[a] Byung Hoon Choi,[a] Hyonseok Hwang,[a] Gyun-Tack Bae,[c] Kang Mun Lee[a,]* and Myung Hwan Park[c,]*

[a] Department of Chemistry, Institute for Molecular Science and Fusion Technology, Kangwon National University, Chuncheon, Gangwon 24341, Republic of Korea

[b] Department of Chemistry, KAIST, Daejeon 34141, Republic of Korea.

[c] Department of Chemistry Education, Chungbuk National University, Cheongju, Chungbuk 28644, Republic of Korea.

Table S1 Crystallographic data and parameters for **6**–**8**.

Compound	**6**·($C_4H_{10}O$)	**7**·($C_4H_{10}O$)	**8**
formula	$C_{51}H_{66}BF_2N_4O_4Al$	$C_{51}H_{64}BF_4N_4O_4Al$	$C_{35}H_{26}BF_2N_4O_3Al$
formula weight	874.87	910.85	626.39
crystal system	Triclinic	Triclinic	Triclinic
space group	$P\bar{1}$	$P\bar{1}$	$P\bar{1}$
a (Å)	11.6723(16)	12.038(2)	10.378(2)
b (Å)	13.9091(16)	14.150(3)	11.375(2)
c (Å)	15.8713(19)	16.086(3)	14.101(3)
α (°)	103.271(7)	102.959(14)	84.83(3)
β (°)	99.123(8)	99.494(14)	71.22(3)
γ (°)	91.663(9)	92.294(14)	86.52(3)
V (Å^3)	2470.4(5)	2625.2(9)	1568.7(5)
Z	2	2	2
ρ_{calc} (g cm^{-3})	1.176	1.152	1.326
μ (mm^{-1})	0.095	0.097	0.119
F(000)	936	968	648
T (K)	296	296	293
hkl range	–13 → +13, –15 → +15, –17 → +17	–11 → +11, –13 → +13, –15 → +13	0 → +14, –16 → +16, –19 → +20
measd reflns	24006	17625	8735
unique reflns [R_{int}]	7360 [0.0796]	5045 [0.0561]	8735 [0.0671]
reflns used for refinement	7360	5045	8735
refined parameters	582	631	418
R1[a] (I > 2σ(I))	0.0532	0.0537	0.0706
wR2[b] all data	0.1634	0.1615	0.2340
GOF on F^2	1.024	1.063	1.031
ρ_{fin} (max/min) (e Å^{-3})	0.498, –0.351	0.257, –0.197	0.786, –0.565

[a] $R1 = \sum||Fo| - |Fc||/\sum|Fo|$. [b] $wR2 = \{[\sum w(Fo^2 - Fc^2)^2]/[\sum w(Fo^2)^2]\}^{1/2}$.

Table S2 Selected bond lengths (Å) and angles (°) for **6**–**8**.

	6	**7**	**8**
		Lengths	
Al–O(1)	1.794(2)	1.788(3)	1.790(15)
Al–O(2)	1.781(2)	1.802(3)	1.800(14)
Al–O(3)	1.757(2)	1.786(3)	1.762(14)
Al–N(1)	2.000(3)	2.003(3)	2.039(16)
Al–N(2)	1.990(3)	2.004(3)	2.057(16)
B–N(3)	1.528(5)	1.545(7)	1.546(3)
B–N(4)	1.536(5)	1.554(7)	1.550(3)
B–F(1)	1.390(4)	1.399(5)	1.383(2)
B–F(2)	1.394(4)	1.392(6)	1.391(2)
O(1)–C(1)	1.321(4)	1.339(4)	1.342(2)
O(2)–C(16)	1.329(4)	1.341(5)	1.339(2)[a]
O(3)–C(33)	1.341(4)	1.350(4)	1.328(2)[b]
		Angles	
O(3)–Al–O(1)	102.30(11)	111.52(14)	120.29(7)
O(3)–Al–O(2)	110.10(11)	101.99(13)	122.68(7)
O(2)–Al–O(1)	91.97(10)	92.39(13)	117.02(7)
O(3)–Al–N(2)	93.88(11)	106.82(14)	94.55(7)
O(2)–Al–N(2)	89.41(11)	89.53(14)	84.38(6)
O(1)–Al–N(2)	162.17(12)	140.27(14)	92.26(6)
O(3)–Al–N(1)	107.86(11)	92.54(13)	93.39(7)
O(2)–Al–N(1)	140.88(11)	163.76(14)	90.28(6)
O(1)–Al–N(1)	88.94(11)	88.94(14)	84.81(6)
N(2)–Al–N(1)	78.91(11)	79.23(15)	171.97(6)
Al–O(1)–C(1)	132.6(2)	135.2(2)	115.84(11)
Al–O(2)–C(16)	134.1(2)	132.6(2)	116.22(11)[c]
Al–O(3)–C(33)	132.2(2)	132.1(3)	132.12(11)[d]
F(1)–B–F(2)	108.2(3)	108.0(4)	109.58(19)
F(1)–B–N(3)	110.7(3)	110.7(4)	110.69(16)
F(2)–B–N(3)	110.0(3)	111.3(4)	110.01(15)
F(1)–B–N(4)	110.6(3)	109.4(4)	110.71(16)
F(2)–B–N(4)	110.5(3)	110.7(4)	110.13(16)
N(3)–B–N(4)	106.8(3)	106.8(4)	105.67(15)

[a] O(2)–C(11), [b] O(3)–C(21), [c] Al–O(2)–C(11), [d] Al–O(3)–C(21).

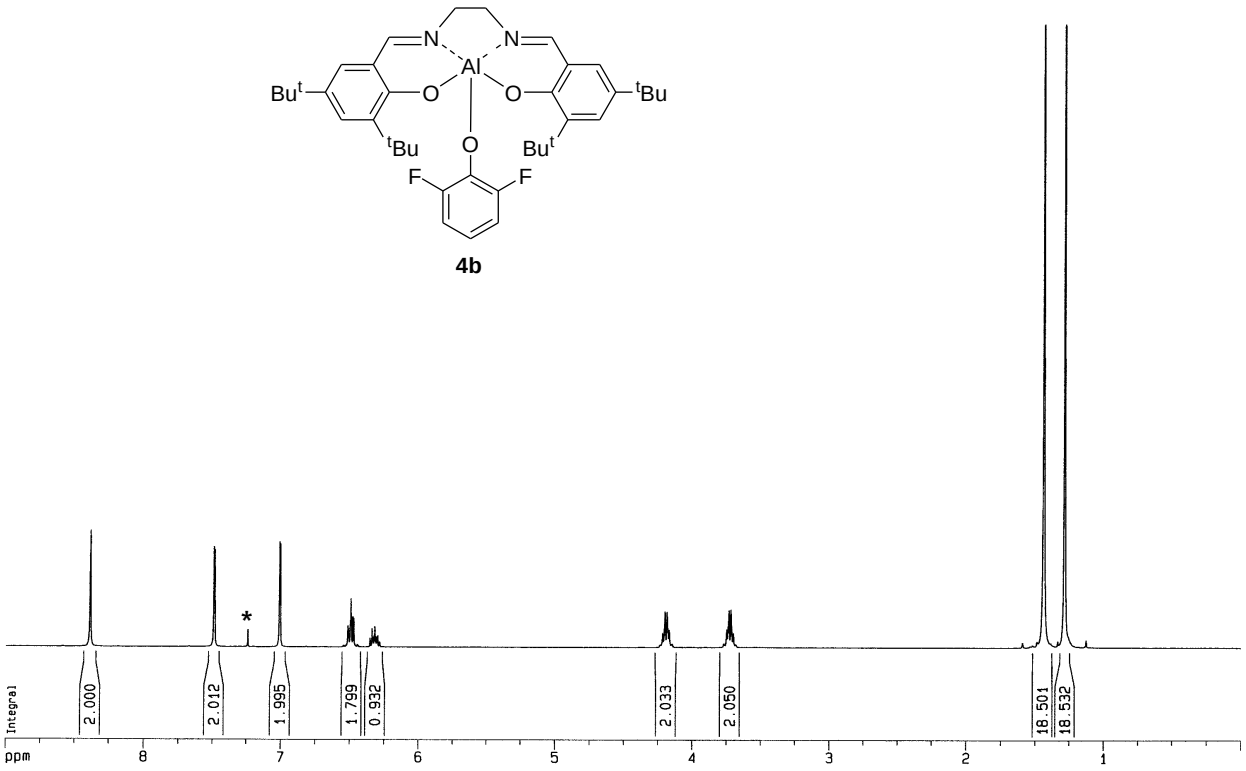

Figure S1. ^{1}H NMR spectra of **4b** (∗ from residual $CHCl_3$ in $CDCl_3$).

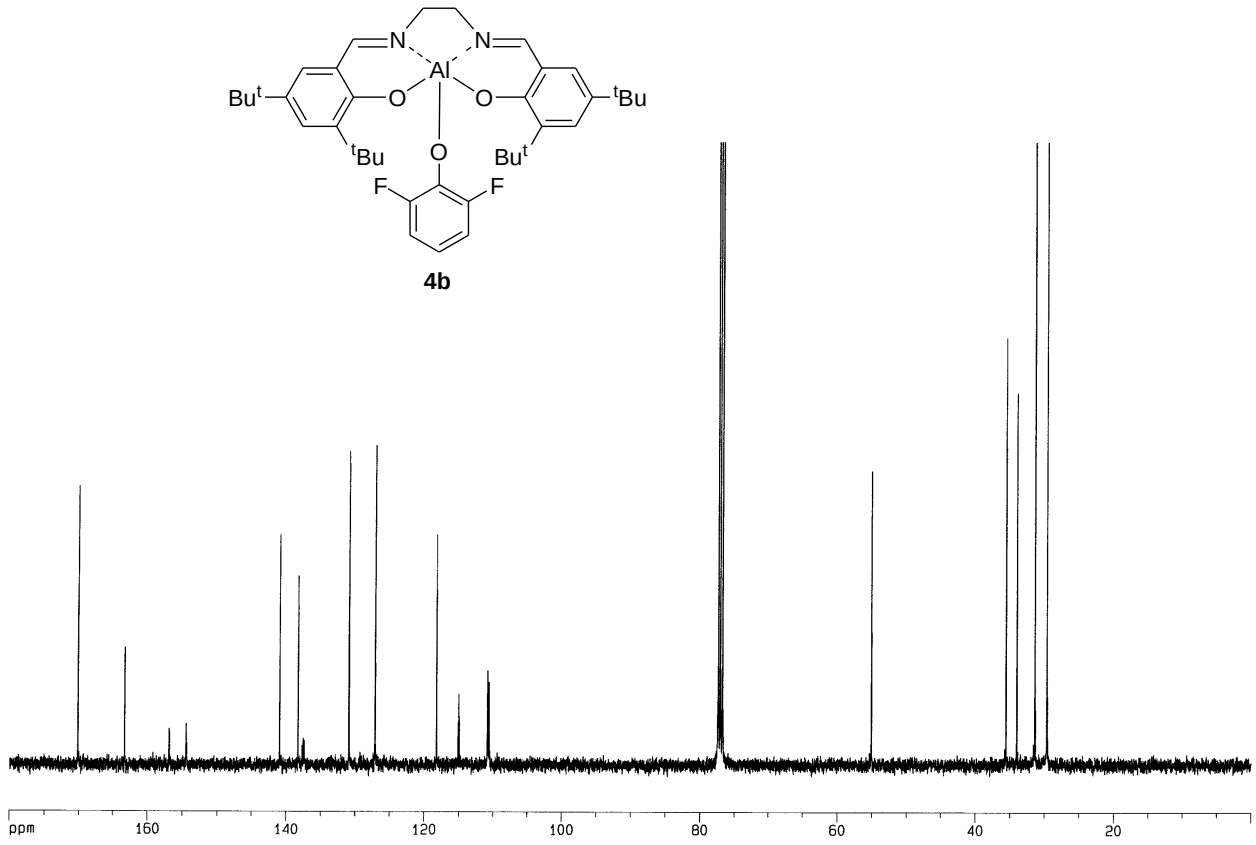

Figure S2. ^{13}C NMR spectra of **4b** in $CDCl_3$.

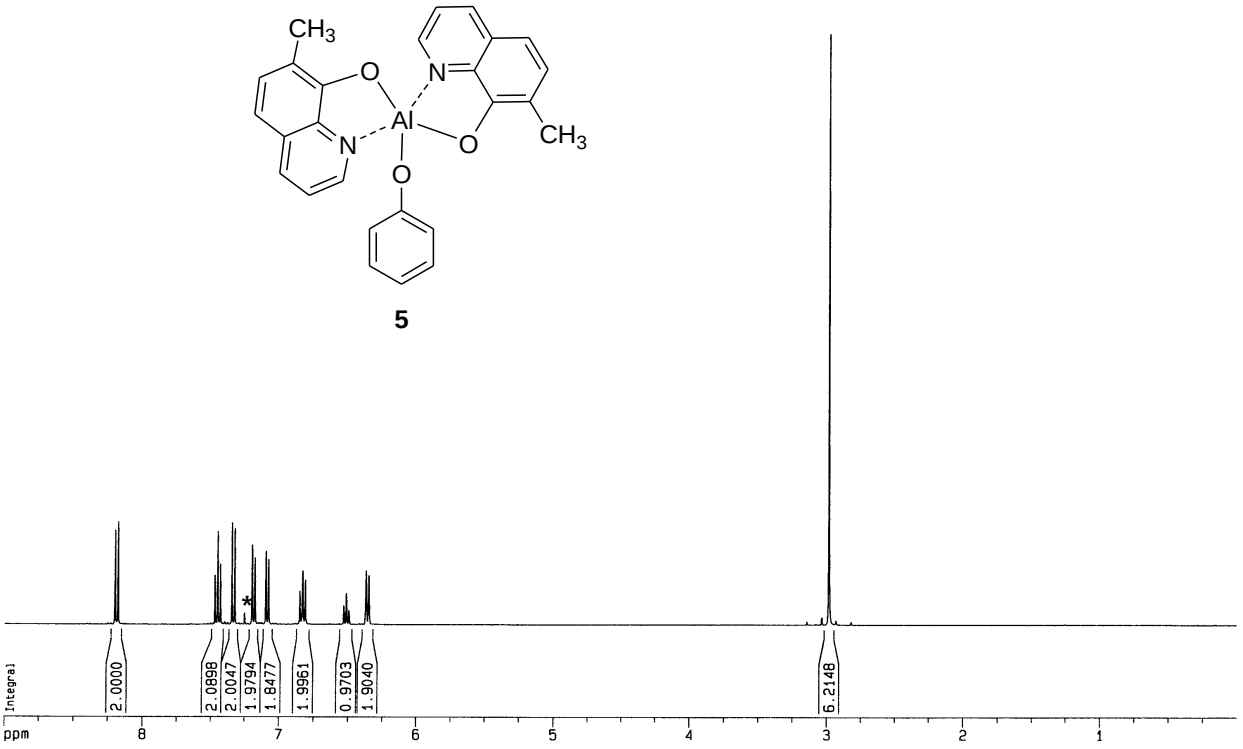

Figure S3. ^{1}H NMR spectra of **5** (∗ from residual $CHCl_3$ in $CDCl_3$).

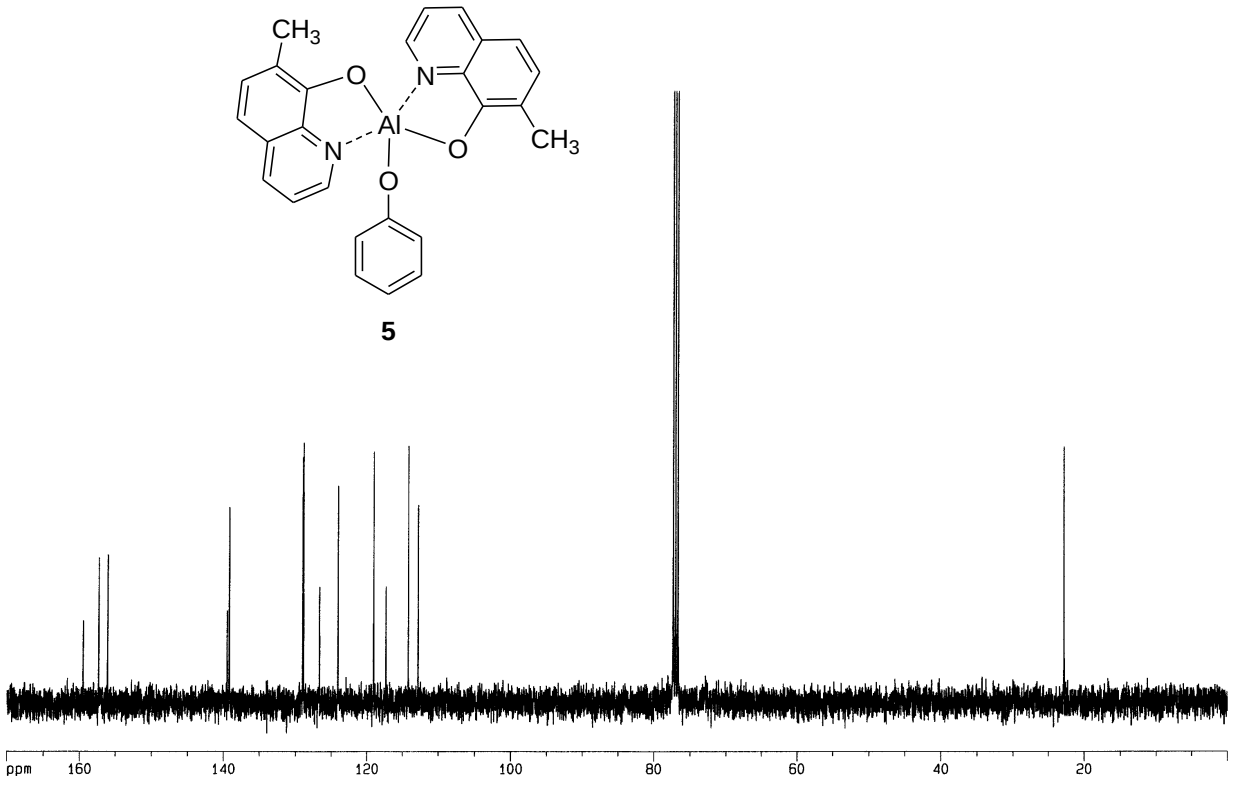

Figure S4. ^{13}C NMR spectra of **5** in $CDCl_3$.

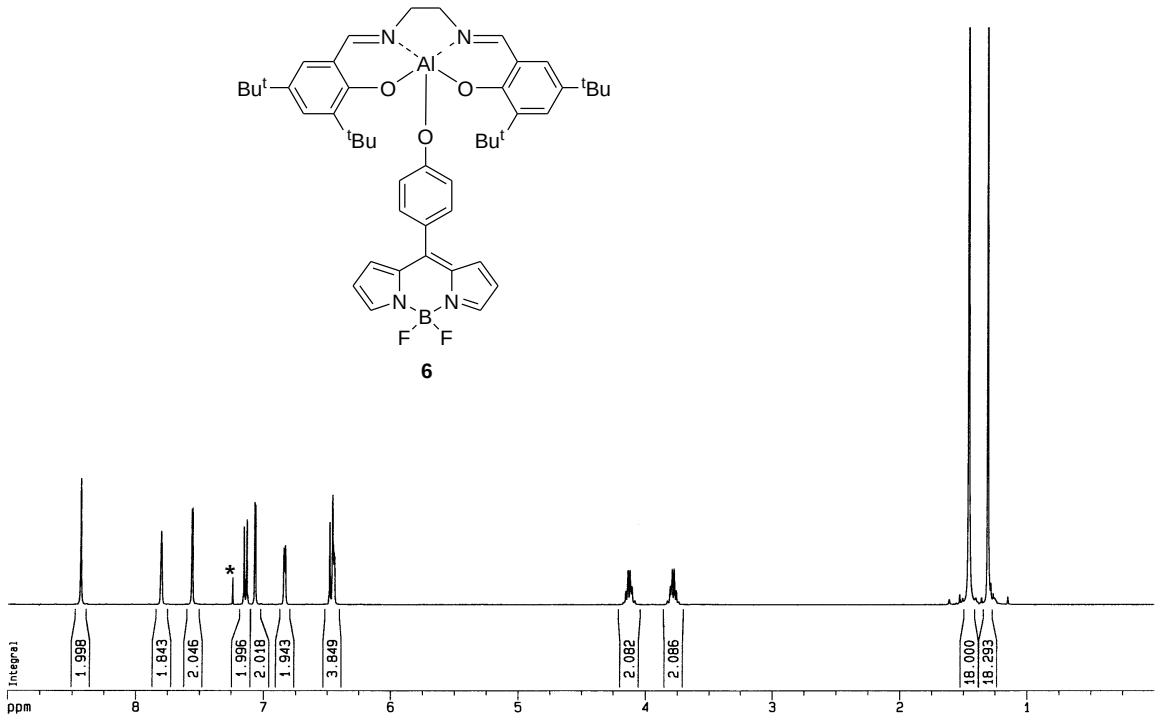

Figure S5. ^{1}H NMR spectra of **6** (∗ from residual $CHCl_3$ in $CDCl_3$).

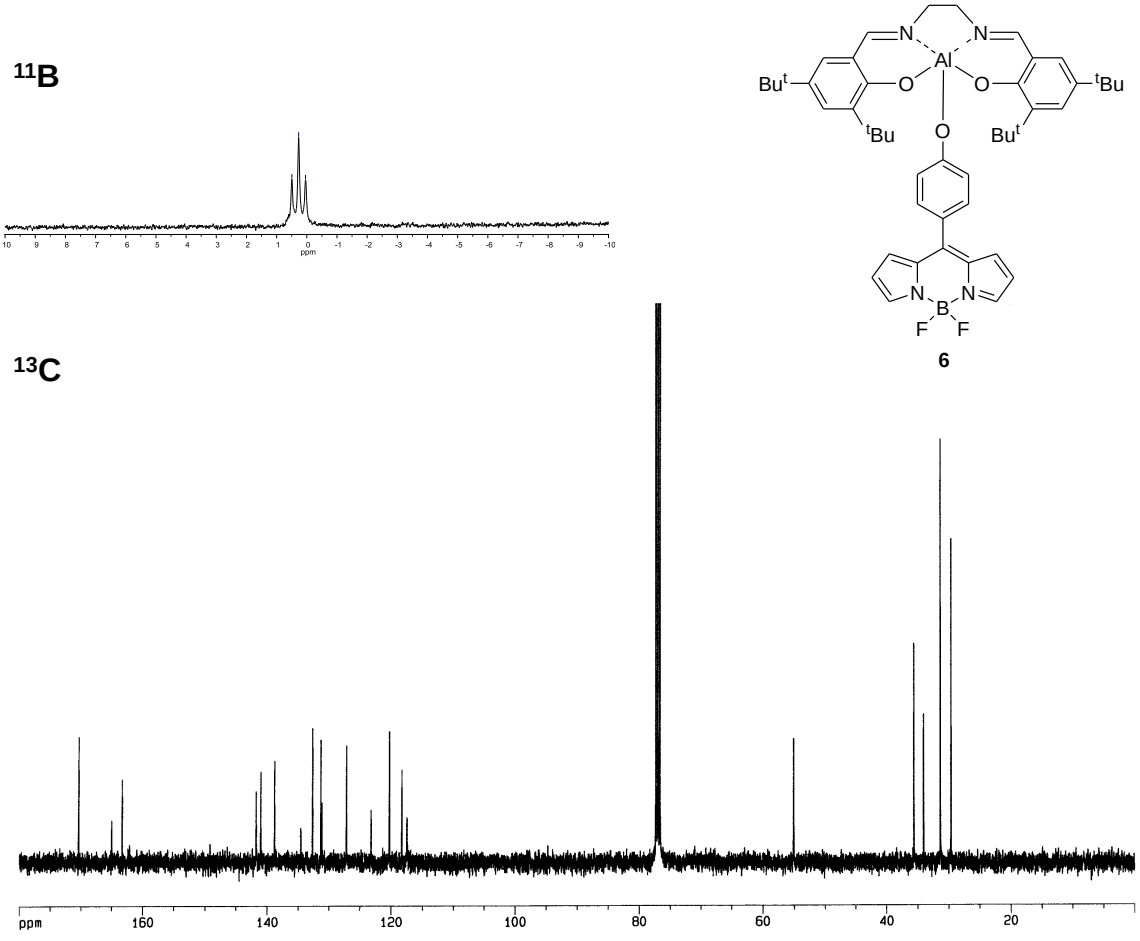

Figure S6. ^{11}B (top) and ^{13}C (bottom) NMR spectra of **6** in $CDCl_3$.

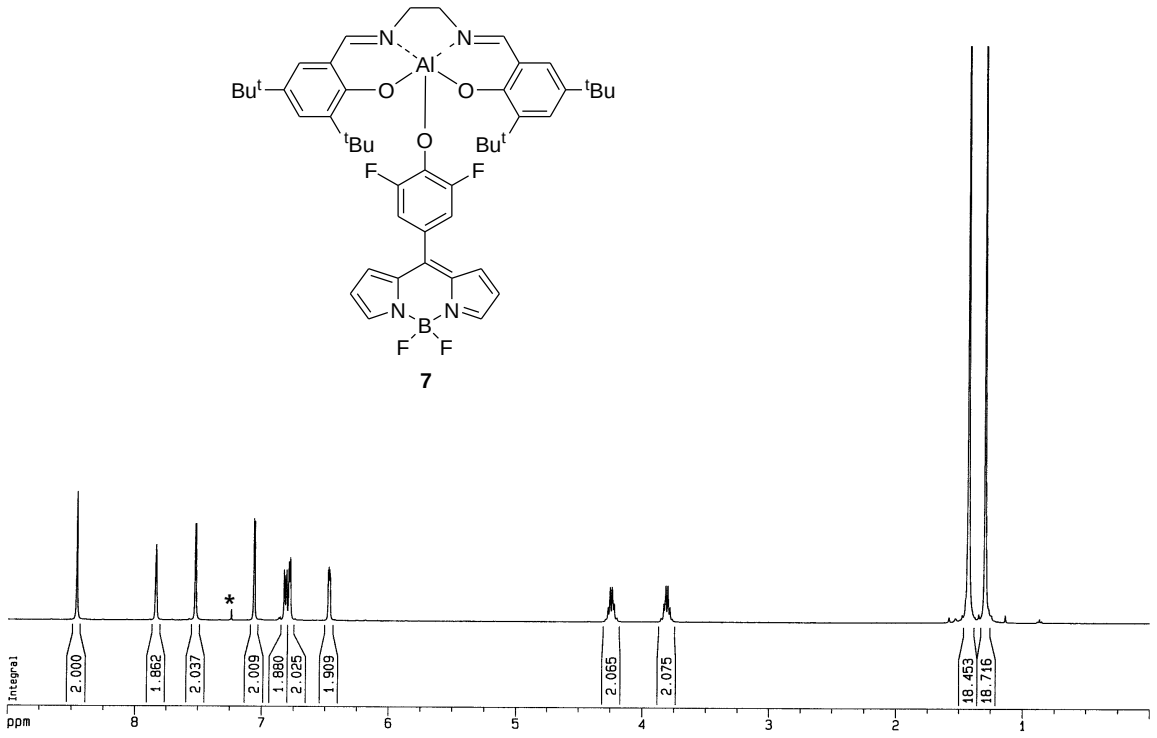

Figure S7. ^{1}H NMR spectra of **7** (∗ from residual $CHCl_3$ in $CDCl_3$).

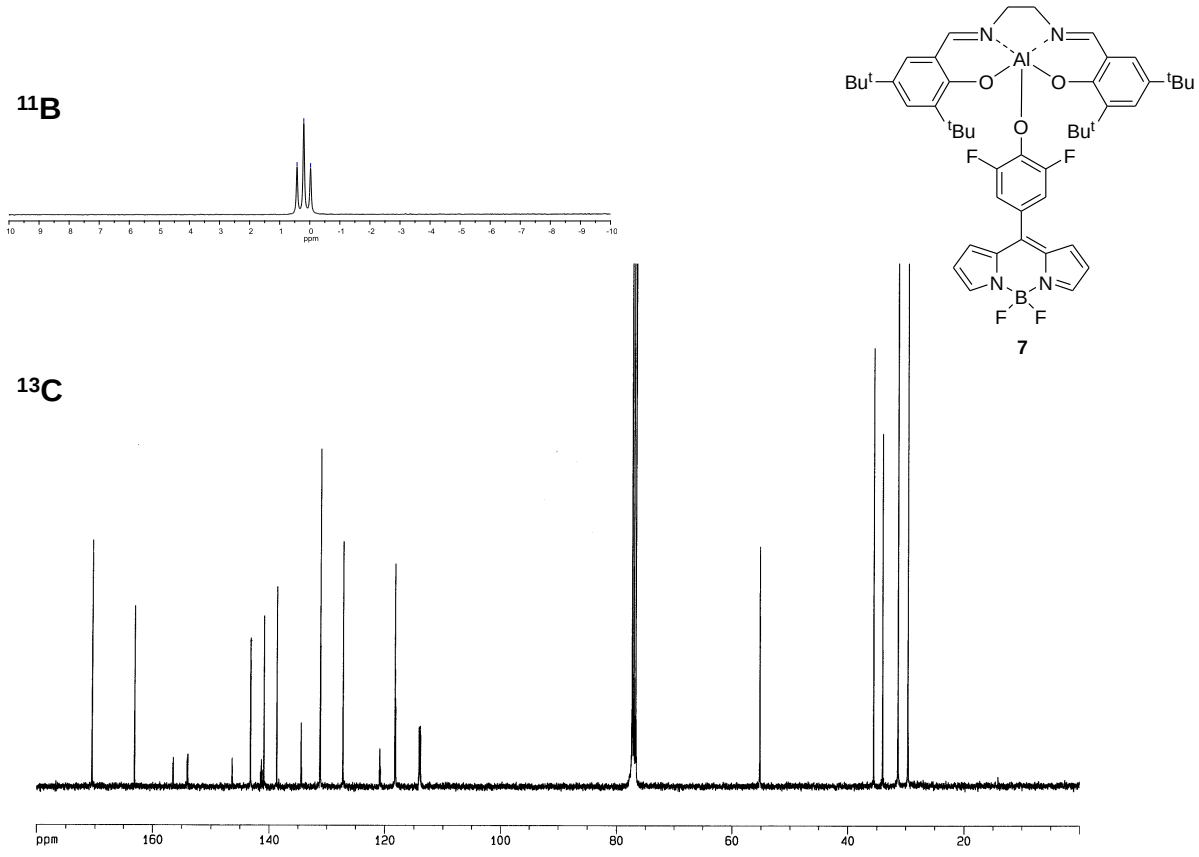

Figure S8. ^{11}B (top) and ^{13}C (bottom) NMR spectra of **7** in $CDCl_3$.

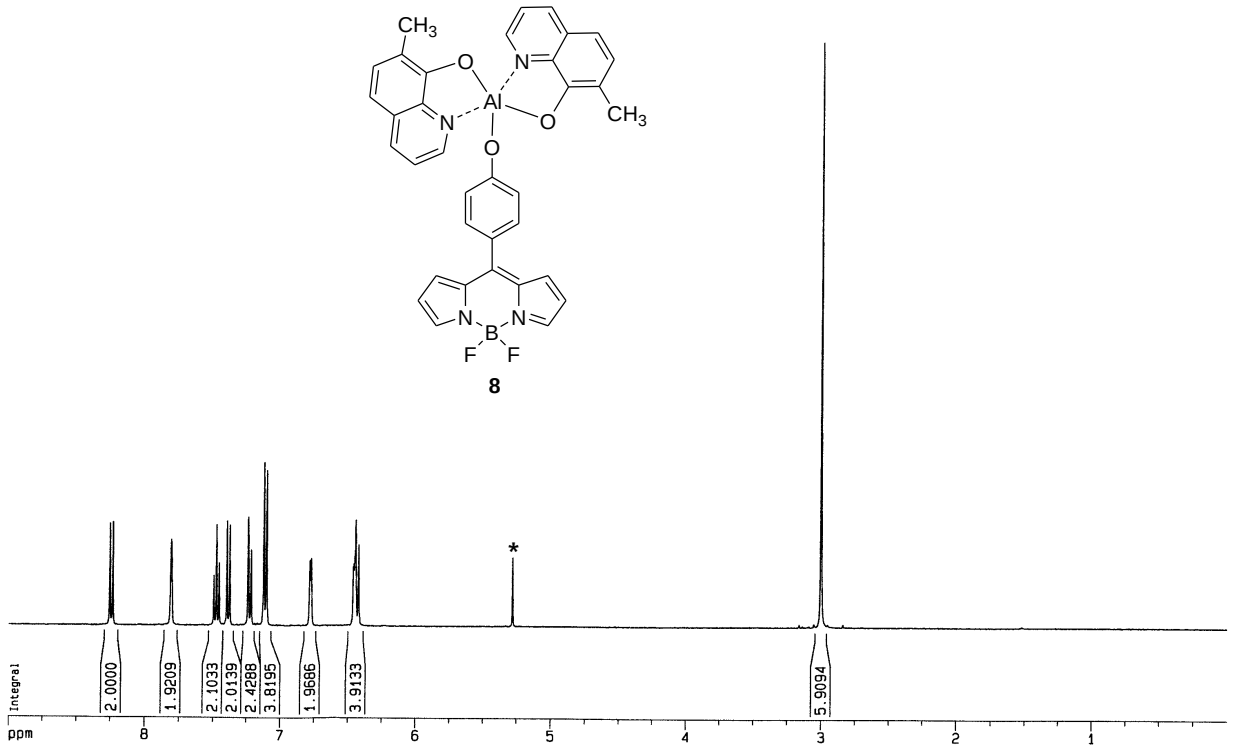

Figure S9. ^{1}H NMR spectra of **8** (∗ from residual $CHCl_3$ in $CDCl_3$).

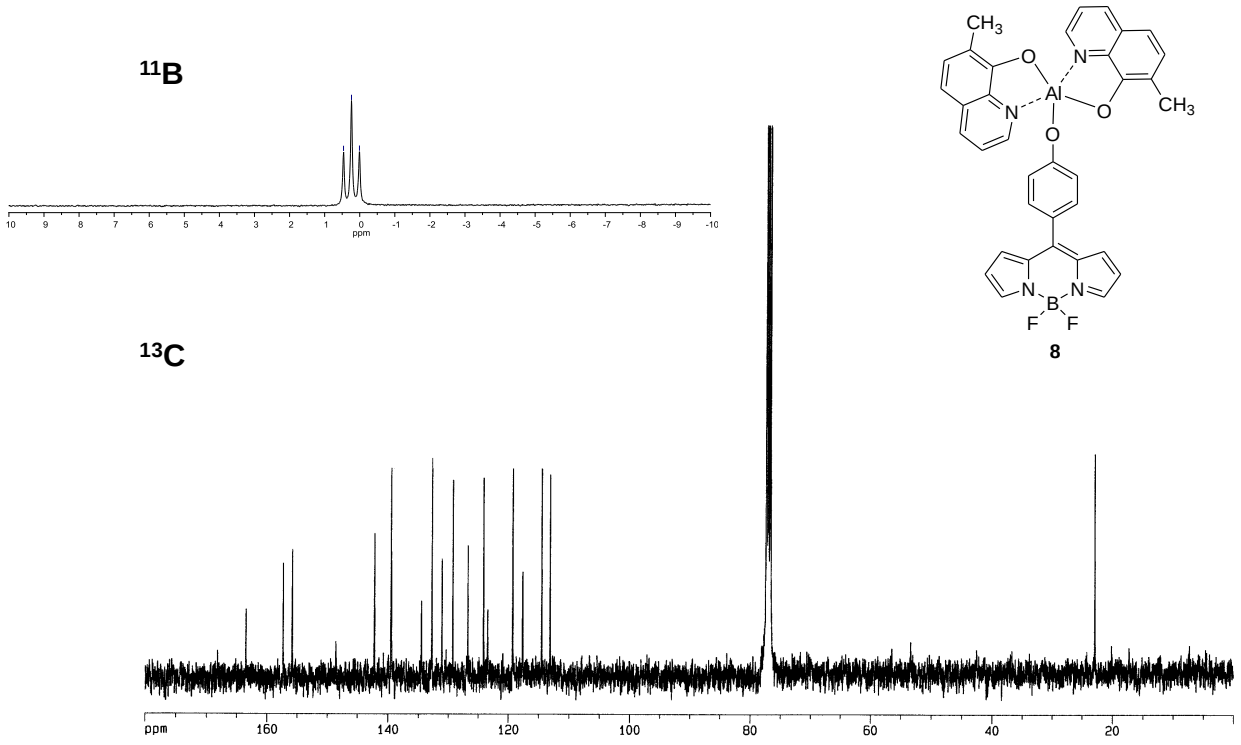

Figure S10. ^{11}B (top) and ^{13}C (bottom) NMR spectra of **8** in $CDCl_3$.

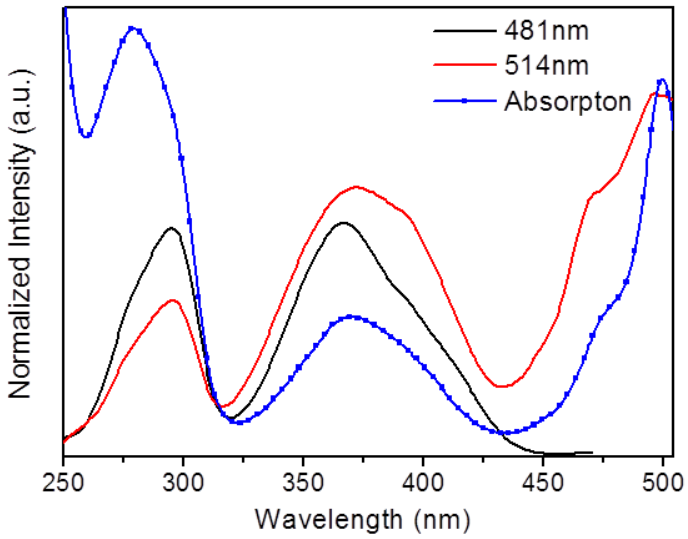

Figure S11. Comparison of absorption (5.0×10^{-5} M) and excitation (5.0×10^{-5} M) spectra for emission of 481 nm and 514 nm for **6** in $CHCl_3$ at room temperature.

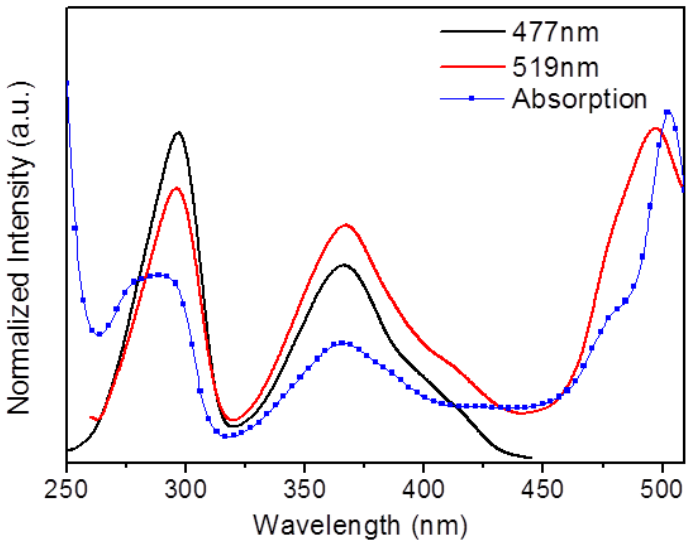

Figure S12. Comparison of absorption (5.0×10^{-5} M) and excitation (5.0×10^{-5} M) spectra for emission of 477 nm and 519 nm for **7** in $CHCl_3$ at room temperature.

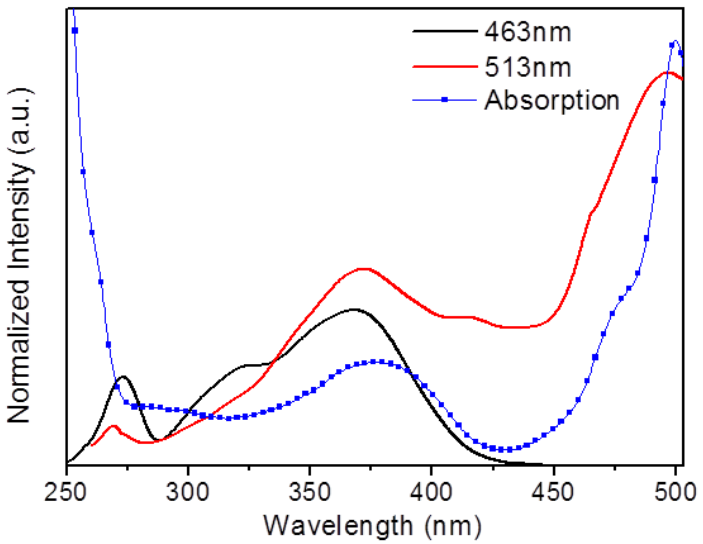

Figure S13. Comparison of absorption (5.0×10^{-5} M) and excitation (5.0×10^{-5} M) spectra for emission of 463 nm and 513 nm for **8** in $CHCl_3$ at room temperature.

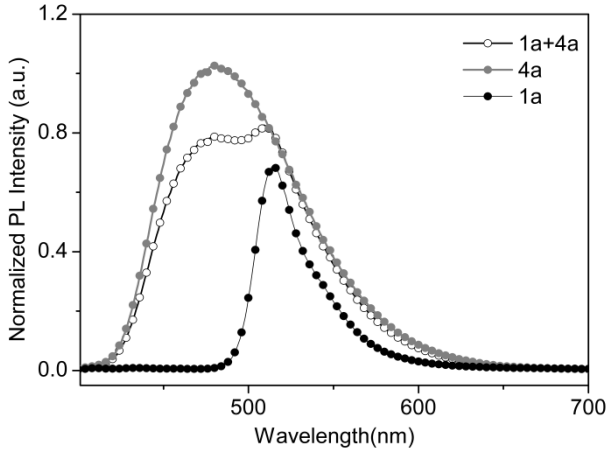

Figure S14. Emission spectra of **1a** (black circle), **4a**, (gray circle) and an equimolar mixture of **1a** and **4a** (open circle) (λ_{ex} = 370nm, 5.0×10^{-5} M, $CHCl_3$).

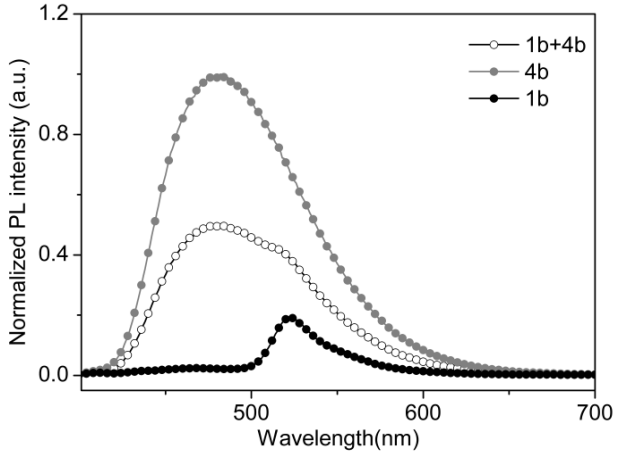

Figure S15. Emission spectra of **1b** (black circle), **4b**, (gray circle) and an equimolar mixture of **1b** and **4b** (open circle) (λ_{ex} = 370nm, 5.0×10^{-5} M, $CHCl_3$).

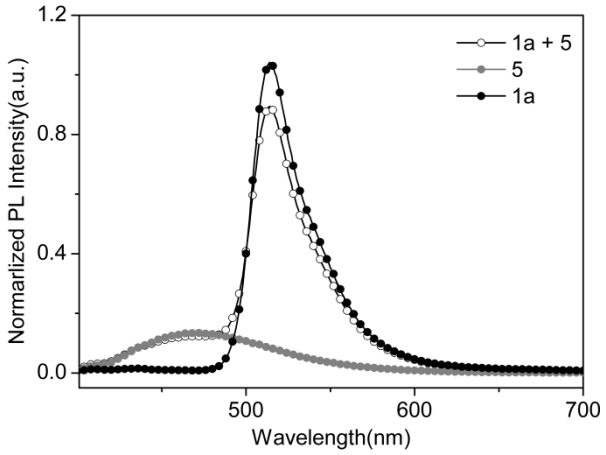

Figure S16. Emission spectra of **1a** (black circle), **5**, (gray circle) and an equimolar mixture of **1a** and **5** (open circle) (λ_{ex} = 370nm, 5.0 × 10^{-5} M, $CHCl_3$).

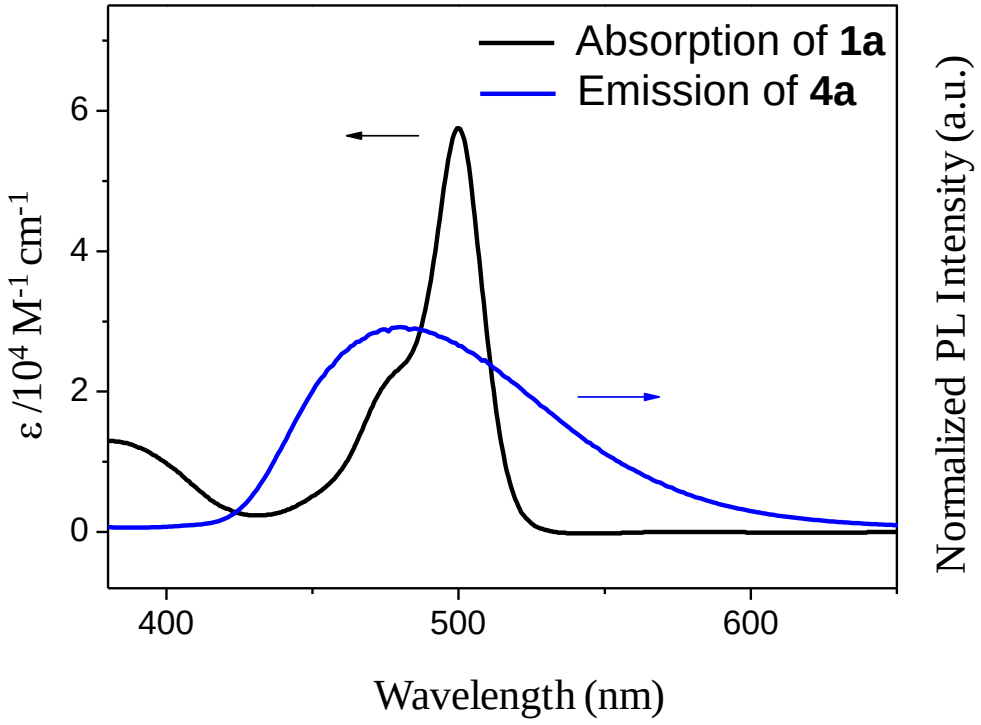

Figure S17. Comparison of absorption spectra of **1a** and emission spectra of **4a** (5.0 × 10^{-5} M, $CHCl_3$).

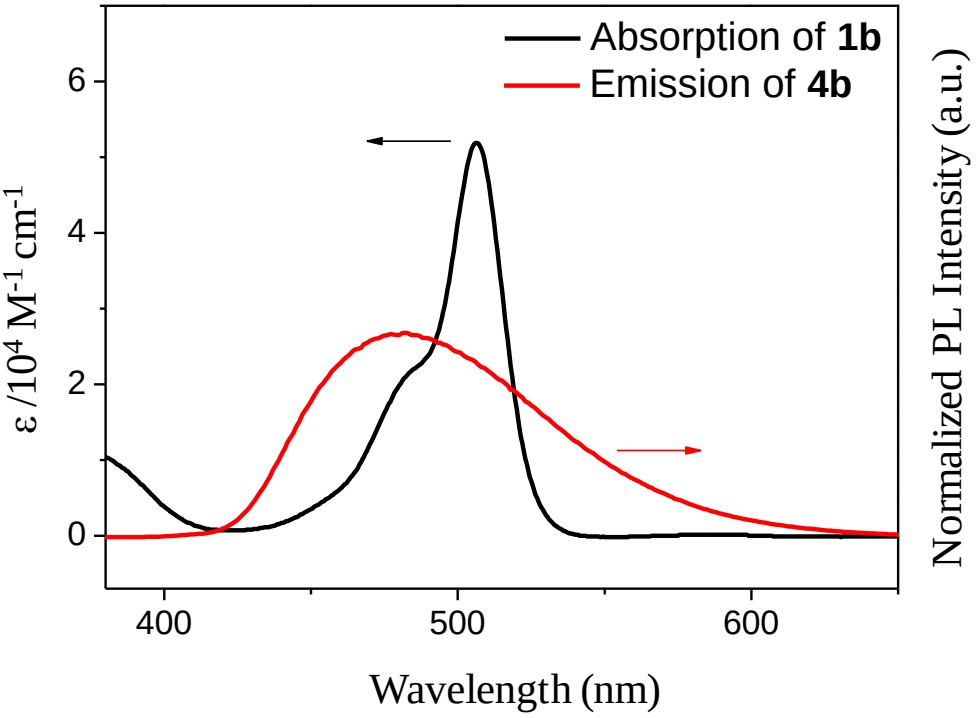

Figure S18. Comparison of absorption spectra of **1b** and emission spectra of **4b** (5.0×10^{-5} M, $CHCl_3$).

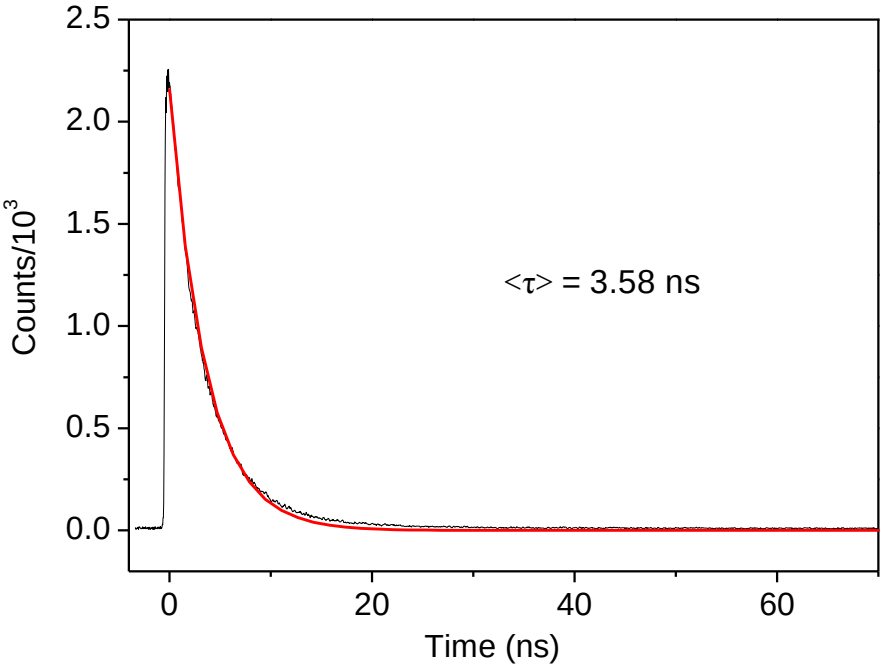

Figure S19. An Emission decay curve detected at 470 nm in $CHCl_3$ (5.0×10^{-5} M) solution of **6** at 298 K (black line). The red-line corresponds to the single-exponential fitting curve (R^2 = 0.9965) for the experimental curve.

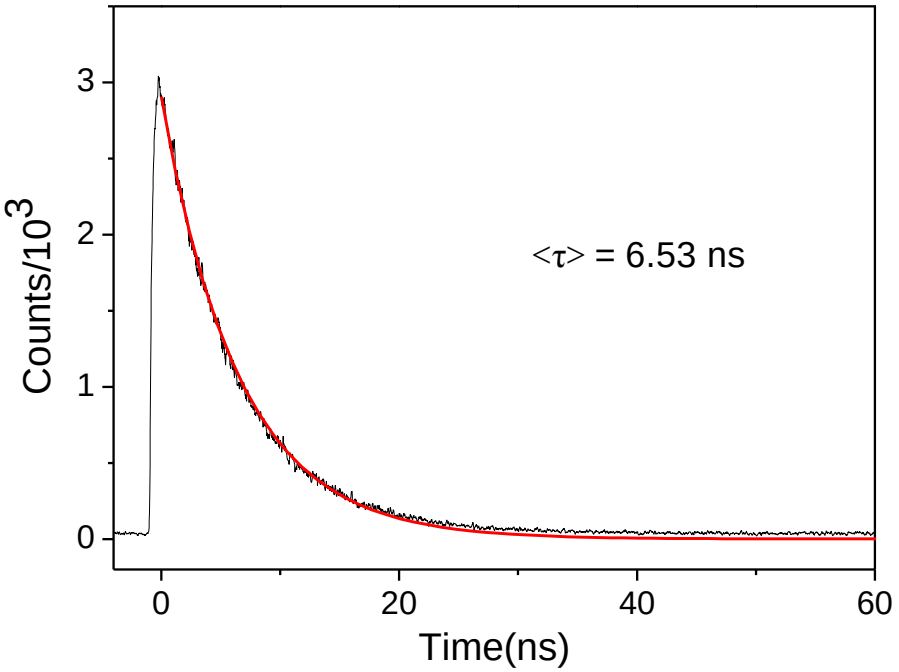

Figure S20. An Emission decay curve detected at 520 nm in $CHCl_3$ (5.0×10^{-5} M) solution of **6** at 298 K (black line). The red-line corresponds to the single-exponential fitting curve (R^2 = 0.9966) for the experimental curve.

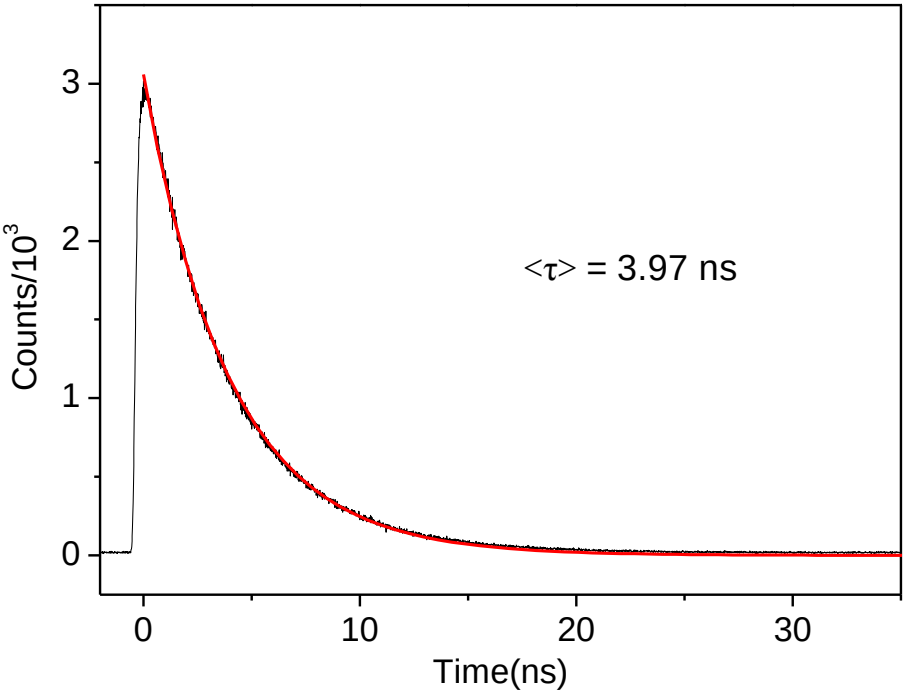

Figure S21. An Emission decay curve detected at 470 nm in $CHCl_3$ (5.0×10^{-5} M) solution of **7** at 298 K (black line). The red-line corresponds to the single-exponential fitting curve (R^2 = 0.9989) for the experimental curve.

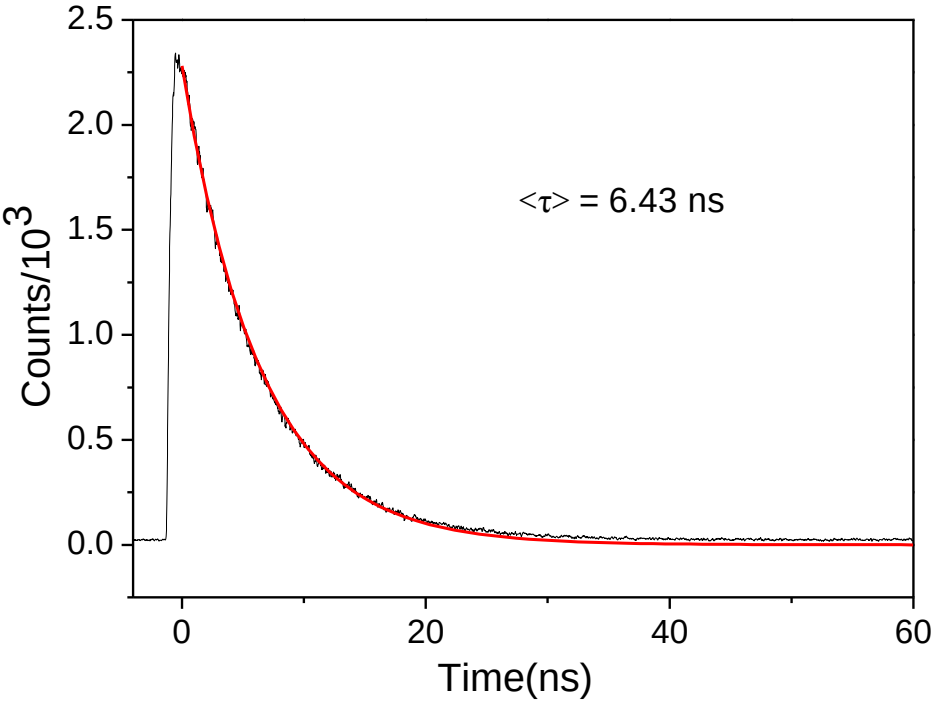

Figure S22. An Emission decay curve detected at 520 nm in $CHCl_3$ (5.0×10^{-5} M) solution of **7** at 298 K (black line). The red-line corresponds to the single-exponential fitting curve ($R^2 = 0.9977$) for the experimental curve.

DFT Computational Results

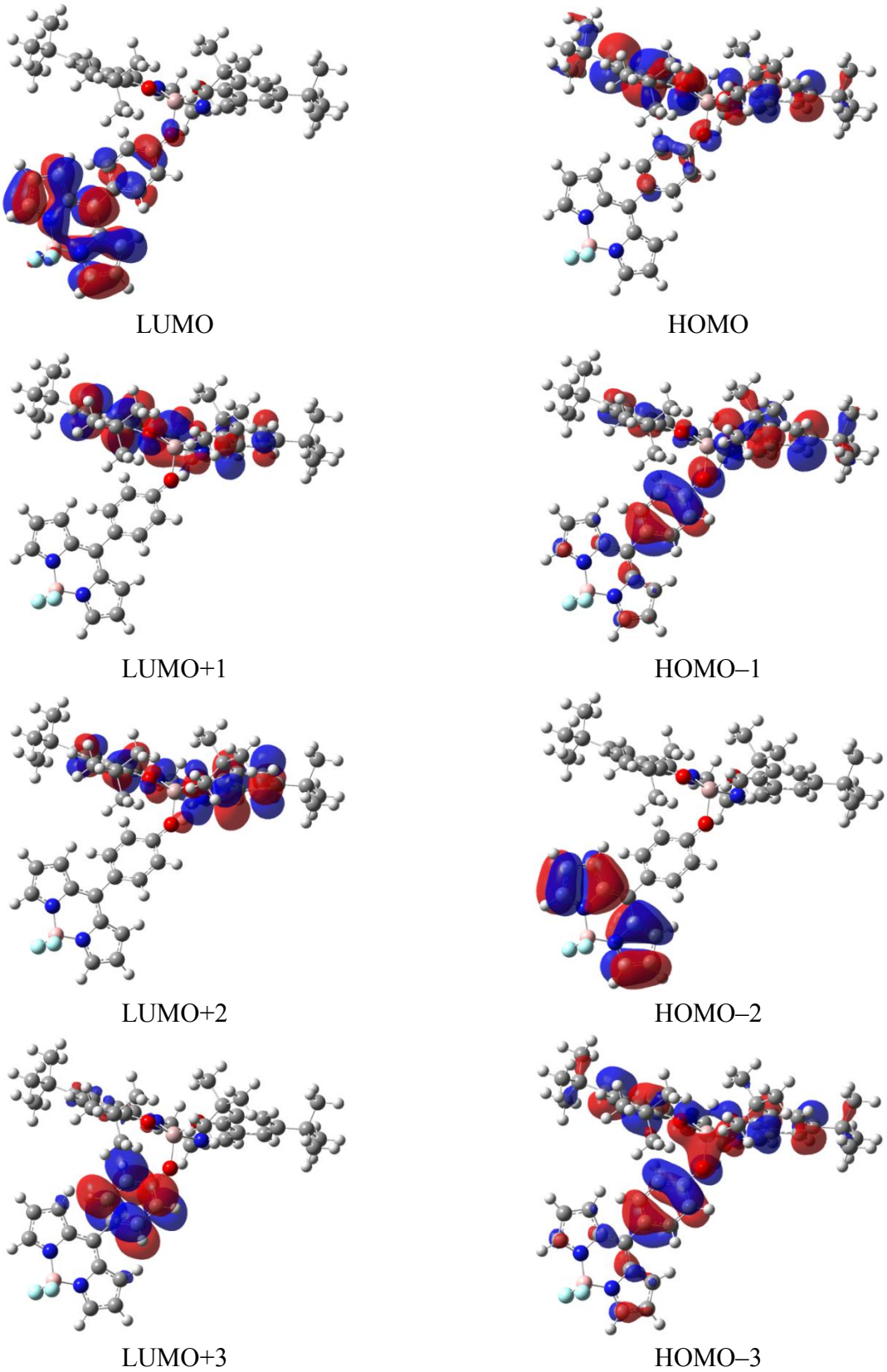

Figure S23. The selected frontier orbitals of **6** from B3LYP/6-31G(d) calculations (Isovalue = 0.04) with CPCM in $CHCl_3$ at their lowest singlet ground state (S_0) optimized geometries.

Table S3 Molecular orbital distributions (in %) and energies (in eV) of **6** at the ground state (S_0) optimized geometries.

Orbitals	Salen-Al	Bridged phenoxy	Bodipy	Energy level
LUMO+4	85.03	13.00	1.97	0.13
LUMO+3	3.20	94.45	2.35	–0.13
LUMO+2	99.69	0.23	0.08	–1.58
LUMO+1	99.19	0.62	0.20	–1.95
LUMO	0.49	11.24	88.28	–2.65
HOMO	93.20	6.05	0.75	–5.65
HOMO–1	56.01	38.17	5.82	–5.77
HOMO–2	0.05	0.65	99.30	–5.81
HOMO–3	51.78	41.36	6.87	–5.91
HOMO–4	99.61	0.34	0.04	–6.68

Table S4 Computed absorption wavelengths (λ_{calc} in nm) and oscillator strengths ($f_{calc.}$) for **6** from TD-B3LYP/6-31G(d) calculations with CPCM in $CHCl_3$ at their lowest singlet ground state (S_0) optimized geometries.

state	λ_{calc} (nm)	$f_{calc.}$	contribution
S1	472.90	0.1366	HOMO–1 → LUMO (17.7%)
			HOMO → LUMO (80.7%)
S2	456.22	0.2169	HOMO–3 → LUMO (22.9%)
			HOMO–1 → LUMO (58.7%)
			HOMO → LUMO (17.9%)
S3	428.25	0.0321	HOMO–3 → LUMO (74.9%)
			HOMO–1 → LUMO (23.3%)
S4	416.05	0.4279	HOMO–6 → LUMO (5.0%)
			HOMO–2 → LUMO (94.8%)
S5	392.99	0.0328	HOMO → LUMO+1 (98.2%)
S6	376.08	0.0207	HOMO–3 → LUMO+1 (2.8%)
			HOMO–1 → LUMO+1 (96.2%)
S7	360.37	0.0551	HOMO–3 → LUMO+1 (94.5%)
			HOMO–1 → LUMO+1 (2.8%)
S8	350.46	0.0482	HOMO–6 → LUMO (59.1%)
			HOMO–2 → LUMO (3.1%)
			HOMO–2 → LUMO+1 (34.7%)
S9	349.40	0.0362	HOMO–6 → LUMO (32.1%)
			HOMO–2 → LUMO+1 (63.4%)
S10	346.04	0.0779	HOMO → LUMO+2 (96.6%)

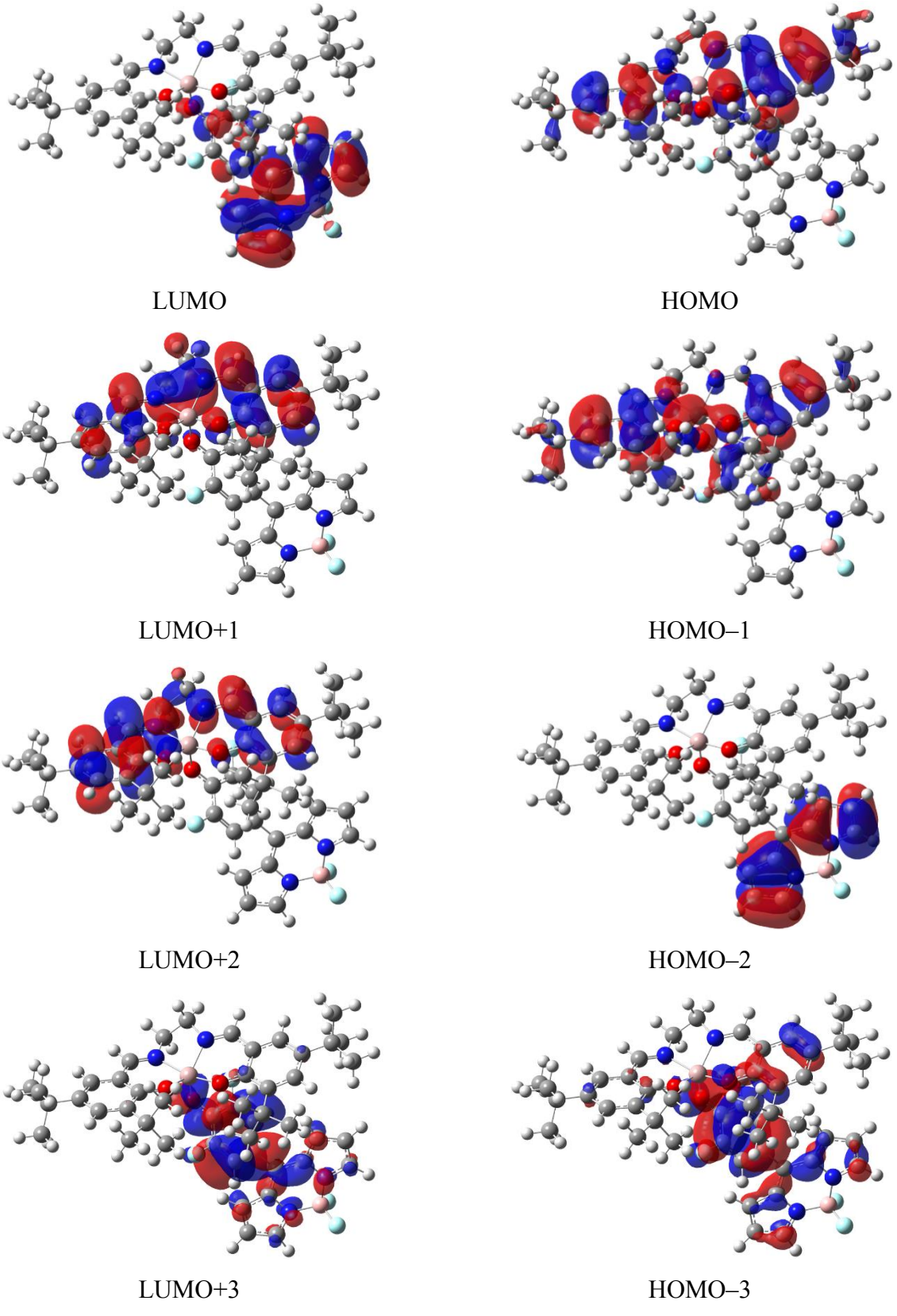

Figure S24. The selected frontier orbitals of **7** from B3LYP/6-31G(d) calculations (Isovalue = 0.04) with CPCM in $CHCl_3$ at their lowest singlet ground state (S_0) optimized geometries.

Table S5 Molecular orbital distributions (in %) and energies (in eV) of **7** at the ground state (S_0) optimized geometries.

Orbitals	Salen-Al	Bridged phenoxy	Bodipy	Energy level
LUMO+4	3.72	94.14	2.14	–0.10
LUMO+3	3.65	84.00	12.35	–0.14
LUMO+2	99.80	0.17	0.03	–1.56
LUMO+1	99.53	0.46	0.01	–1.89
LUMO	0.21	9.96	89.83	–2.79
HOMO	96.41	3.31	0.27	–5.63
HOMO–1	91.55	7.62	0.83	–5.81
HOMO–2	0.06	0.75	99.19	–5.91
HOMO–3	13.82	76.25	9.93	–6.12
HOMO–4	99.28	0.65	0.07	–6.66

Table S6 Computed absorption wavelengths (λ_{calc} in nm) and oscillator strengths ($f_{calc.}$) for **7** from TD-B3LYP/6-31G(d) calculations with CPCM in $CHCl_3$ at their lowest singlet ground state (S_0) optimized geometries.

state	λ_{calc} (nm)	$f_{calc.}$	contribution
S1	504.92	0.0219	HOMO–1 → LUMO (5.2%)
			HOMO → LUMO (94.6%)
S2	461.46	0.0649	HOMO–3 → LUMO (5.1%)
			HOMO–1 → LUMO (89.4%)
			HOMO → LUMO (5.3%)
S3	435.08	0.2098	HOMO–3 → LUMO (94.2%)
			HOMO–1 → LUMO (5.2%)
S4	419.91	0.4338	HOMO–7 → LUMO (5.5%)
			HOMO–2 → LUMO (94.7%)
S5	388.53	0.0216	HOMO → LUMO+1 (98.1%)
S6	368.22	0.0072	HOMO–6 → LUMO (94.0%)
			HOMO–5 → LUMO (3.6%)
S7	363.09	0.069	HOMO–1 → LUMO+1 (97.1%)
S8	350.95	0.0239	HOMO–7 → LUMO (17.7%)
			HOMO–6 → LUMO (2.9%)
			HOMO–5 → LUMO (16.3%)
			HOMO–4 → LUMO (61.6%)
S9	349.63	0.0848	HOMO–7 → LUMO (75.5%)
			HOMO–5 → LUMO (2.1%)
			HOMO–4 → LUMO (17.5%)
			HOMO–2 → LUMO (4.5%)

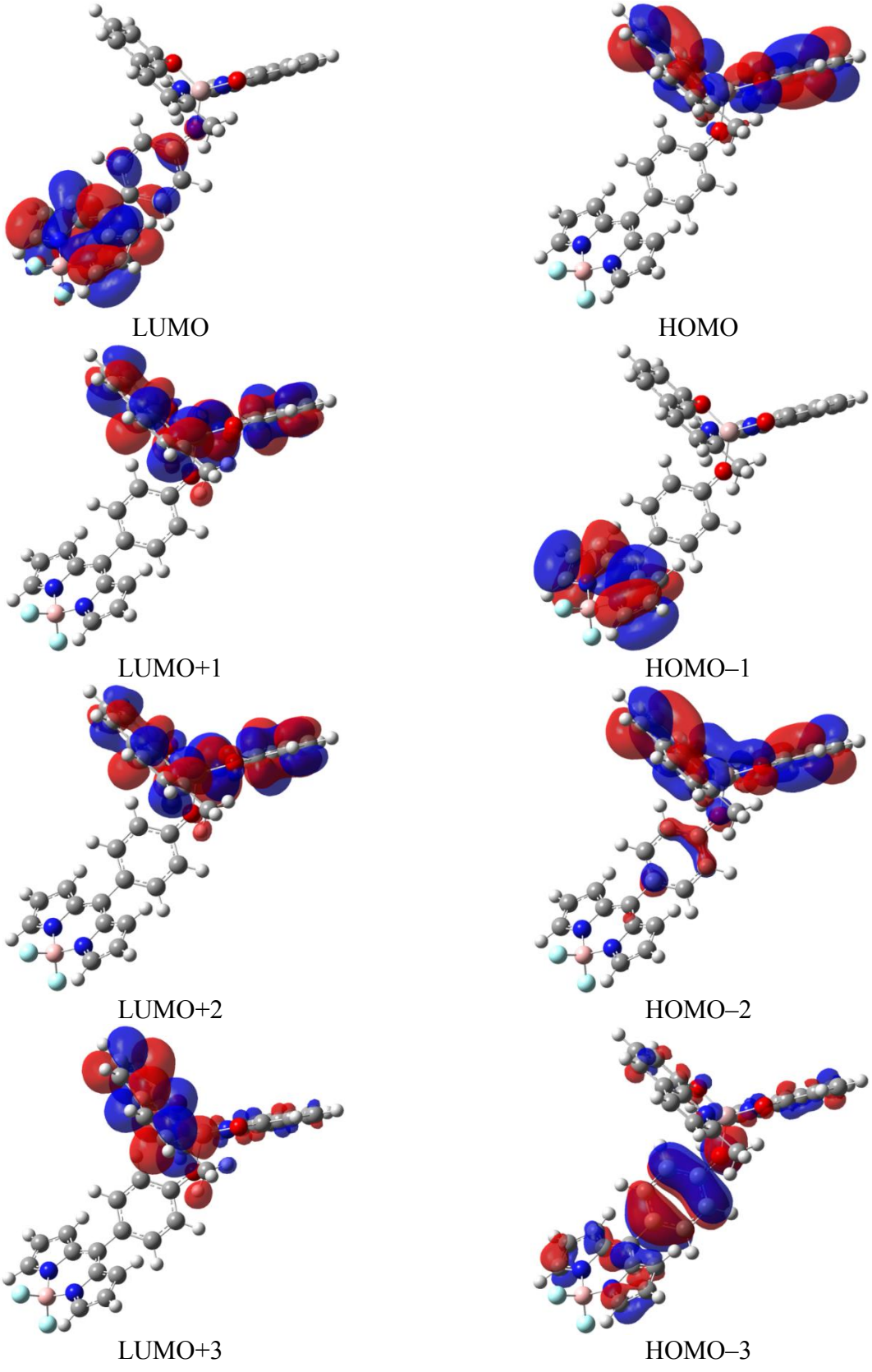

Figure S25. The selected frontier orbitals of **8** from B3LYP/6-31G(d) calculations (Isovalue = 0.04) with CPCM in $CHCl_3$ at their lowest singlet ground state (S_0) optimized geometries.

Table S7 Molecular orbital distributions (in %) and energies (in eV) of **8** at the ground state (S_0) optimized geometries.

Orbitals	Salen-Al	Bridged phenoxy	Bodipy	Energy level
LUMO+4	99.81	0.17	0.01	–0.65
LUMO+3	99.60	0.38	0.02	–0.69
LUMO+2	99.75	0.24	0.00	–1.84
LUMO+1	99.86	0.13	0.01	–1.91
LUMO	0.17	10.75	89.08	–2.70
HOMO	99.34	0.62	0.04	–5.72
HOMO–1	0.18	0.60	99.22	–5.86
HOMO–2	92.18	6.70	1.11	–5.90
HOMO–3	9.80	78.09	12.11	–5.96
HOMO–4	0.15	5.84	94.01	–6.88

Table S8 Computed absorption wavelengths (λ_{calc} in nm) and oscillator strengths ($f_{calc.}$) for **8** from TD-B3LYP/6-31G(d) calculations with CPCM in $CHCl_3$ at their lowest singlet ground state (S_0) optimized geometries.

state	λ_{calc} (nm)	$f_{calc.}$	contribution
S1	458.93	0.0063	HOMO–2 → LUMO (2.3%)
			HOMO → LUMO (95.9%)
S2	448.99	0.3555	HOMO–3 → LUMO (81.0%)
			HOMO–2 → LUMO (17.9%)
S3	429.26	0.0064	HOMO–3 → LUMO (16.5%)
			H OMO–2 → LUMO (79.4%)
			HOMO → LUMO (3.8%)
S4	416.26	0.4319	HOMO–4 → LUMO (5.4%)
			HOMO–1 → LUMO (94.7%)
S5	384.33	0.1114	HOMO–2 → LUMO+2 (6.9%)
			HOMO → LUMO+1 (89.0%)
			HOMO → LUMO+2 (2.1%)
S6	375.07	0.0025	HOMO–2 → LUMO+1 (14.9%)
			HOMO → LUMO+2 (80.7%)
S7	359.38	0.0042	HOMO–3 → LUMO+1 (2.2%)
			HOMO–2 → LUMO+1 (76.7%)
			HOMO–2 → LUMO+2 (5.0%)
			HOMO → LUMO+1 (2.2%)
			HOMO → LUMO+2 (15.6%)
S8	354.15	0.0011	HOMO–3 → LUMO+1 (72.2%)
			HOMO–3 → LUMO+2 (9.1%)

			HOMO–2 → LUMO+1 (3.9%)
			HOMO–2 → LUMO+2 (11.5%)
			HOMO → LUMO+2 (2.7%)
S9	352.92	0.0036	H OMO–3 → LUMO+1 (11.1%)
			HOMO–3 → LUMO+2 (4.2%)
			HOMO–2 → LUMO+1 (2.5%)
			HOMO–2 → LUMO+2 (74.5%)
			HOMO → LUMO+1 (6.2%)
S10	349.87	0.0959	HOMO–4 → LUMO (93.5%)
			HOMO–1 → LUMO (5.3%)